Received: 3 March 2020 | Revised: 18 June 2020 | Accepted: 19 June 2020

DOI: 10.1096/fj.202000467R

RESEARCH ARTICLE

THE FASEB JOURNAL

Thymopentin improves the survival of septic mice by promoting the production of 15-deoxy-prostaglandin J2 and activating the PPARγ signaling pathway

Ye Zhang[1] | Xue Yang[1] | Wenchao Yan[1] | Rui Li[1] | Qian Ye[1] | Linjun You[1] | Wenhao Xie[1] | Kun Mo[1] | Ruifeng Fu[1] | Yanxiang Wang[1] | Yufei Chen[1] | Hui Hou[1] | Yong Yang[1] | Lutz Birnbaumer[2] | Qin Di[3] | Xianjing Li[1]

[1]Center for New Drug Safety Evaluation and Research, State Key Laboratory of Natural Medicines, China Pharmaceutical University, Nanjing, China

[2]Institute of Biomedical Research (BIOMED), Catholic University of Argentina, Buenos Aires, Argentina

[3]School of Sports and Health, Nanjing Sport Institute, Nanjing, China

Correspondence
Lutz Birnbaumer, Institute of Biomedical Research (BIOMED), Catholic University of Argentina, Buenos Aires C1107AFF, Argentina.
Email: birnbau1@gmail.com

Di Qin, School of Sports and Health, Nanjing Sport Institute, Nanjing 210014, P.R. China.
Email: sindyshu@163.com

Xianjing Li, State Key Laboratory of Natural Medicines, Center for New Drug Safety Evaluation and Research, China Pharmaceutical University, Nanjing 210009, P.R. China.
Email: xjl@cpu.edu.cn

Funding information
Basic Research Program of Jiangsu Province, Grant/Award Number: BK20170732; National Natural Science Foundation of China, Grant/Award Number: 81703562, 81571984 and 81703563

Abstract

Sepsis, a systemic inflammatory response syndrome (SIRS) caused by infection, is a major public health concern with limited therapeutic options. Infection disturbs the homeostasis of host, resulting in excessive inflammation and immune suppression. This has prompted the clinical use of immunomodulators to balance host response as an alternative therapeutic strategy. Here, we report that Thymopentin (TP5), a synthetic immunomodulator pentapeptide (Arg-Lys-Asp-Val-Tyr) with an excellent safety profile in the clinic, protects mice against cecal ligation and puncture (CLP)-induced sepsis, as shown by improved survival rate, decreased level of pro-inflammatory cytokines and reduced ratios of macrophages and neutrophils in spleen and peritoneum. Regarding mechanism, TP5 changed the characteristics of LPS-stimulated macrophages by increasing the production of 15-deoxy-$\Delta^{12,14}$-prostaglandin J2 (15-d-PGJ2). In addition, the improved effect of TP5 on survival rates was abolished by the peroxisome proliferator-activated receptor γ (PPARγ) antagonist GW9662. Our results uncover the mechanism of the TP5 protective effects on CLP-induced sepsis and shed light on the development of TP5 as a therapeutic strategy for lethal systemic inflammatory disorders.

KEYWORDS

15-d-PGJ2, macrophage, PPARγ, thymopentin, sepsis

Abbreviations: 15-d-PGJ2, 15-deoxy-$\Delta^{12,14}$-prostaglandin J2; AA, arachidonic acid; CLP, cecal ligation and puncture; HPGDS, hematopoietic prostaglandin D synthase; IL-1, interleukin 1; IL-6, interleukin 6; IL-10, interleukin 10; LPS, lipopolysaccharide; NO, nitric oxide; PPARγ, peroxisome proliferator-activated receptor γ; SOD, superoxide dismutase; TGF-β, transforming growth factor-β; TNF-α, tumor necrosis factor alpha; TP5, Thymopentin.

Ye Zhang and Xue Yang contributed equally to the present study.

1 | INTRODUCTION

Despite the rapid development of medical technology, sepsis is still one of the most elusive syndromes and manifests as a life-threatening disease. In a recent Edition of International Consensus Definitions (Sepsis 3.0), sepsis is defined as an organ dysfunction that is caused by a dysregulated host response to infection.[1] For many years, an unbalanced inflammatory response to complicated infection was considered to be crucial in the pathogenesis of sepsis, but it is now clear that the host response is destroyed in a much more complicated way, which includes durative excessive inflammation and immune suppression, and finally a failure to return to normal homeostasis.[2] Cellular metabolism has a direct role in regulating cell function and emerged as a key mechanism by which inflammatory responses are regulated.[3] The imbalance in cellular metabolic processes has an essential role in immune paralysis of sepsis. Thus, identification and development of pharmacological targets of key cellular metabolism regulators that control the overwhelming immune response could be useful for sepsis therapy.

Thymopoietin (TP) is a polypeptide composed of 49 amino acids residues isolated from bovine thymus, secreted mainly by the epithelial cells of the thymic cortex and medulla. Thymopentin (TP5) is a synthetic pentapeptide (Arg-Lys-Asp-Val-Tyr, Mw = 679.77) based on the active sites of TP (32 ~ 36 amino acid residues) that possesses most of the biological activity of TP.[4] As an approved drug in China, TP5 has been widely used in clinic for immune enhancement and treatment of immune-related diseases such as acquired immunodeficiency syndrome (AIDS), cancers, and autoimmune diseases. It balances the immune system without observable side effects, even at very high doses.[5] However, little is known about the function and molecular mechanism of TP5 against sepsis.

This study was designed to investigate the functional effect and mechanism of TP5 action in sepsis, and particularly with regard to regulation of metabolism associated with inflammation.

2 | MATERIALS AND METHODS

2.1 | Animals

Male C57BL/6N wild-type mice (weighing 18 ~ 22 g, 6 ~ 8 weeks old) were purchased from Beijing Vital River Laboratory Animal Technology Co., Ltd and were acclimatized before use for at least one week in their cages (six mice per cage) under specific conditions (12 hours light-dark cycle, 18°C ~ 22°C, 40% ~ 60% humidity) with unlimited access to regular food and water. All animal experiments were performed in accordance with the National Institutes of Health Guide for the Care and Use of Laboratory Animals and were approved by the Ethics Committee for Animal Experimentation of the Center for New Drug Safety Evaluation and Research of China Pharmaceutical University.

2.2 | Animal sepsis model

First, mice were randomly divided into the following four groups: (a) control (normal mice without operation were injected with normal saline (NS)); (b) sham operation (mice were injected with NS after abdominal operation without ligation and puncture of the cecum; (c) cecal ligation and puncture (CLP)+NS; and (d) CLP+TP5. Then, the mouse CLP sepsis model was established following previous publications.[6] Briefly, C57BL/6N mice were anesthetized via 2.5% of isoflurane inhalation. A midline abdominal incision was made after abdominal shaving and disinfection with 75% of ethanol. The cecum was exteriorized, ligated at 50% of its length with a 4/0 silk thread, and subsequently punctured twice through-and-through with a 21-gauge needle. A small drop of intestinal contents was extruded from the puncture holes. Then, the surface of the cecum was cleaned without leaving any residue on it. The ligated cecum was repositioned into the abdominal cavity, and the abdomen was closed in layers with 5/0 ETHILON sutures (the abdominal wall and skin were sutured in layers with 4-0 silk). After disinfection of the abdomen with iodine, mice received NS (10 mg/kg subcutaneously (s.c.)) or TP5 (10 mg/kg s.c.) after 0.5 hour and were put back into the cage with medical gauze.

2.3 | Animal anatomy and specimen processing

Orbital blood was collected in 3 mL heparin sodium blood collection tubes, centrifuged at 300 g for 10 minutes at 4°C. The plasma of each sample was divided into 20 μL aliquots for routine blood analysis and inflammatory factor detection. A total of 5 mL NS was injected into the abdominal cavity of mice, and the abdomen of mice was rubbed repeatedly. The abdominal cavity fluid was collected and centrifuged at 300 g for 3 minutes, the upper suspension was discarded and peritoneal cells were suspended with 100 μL of phosphate buffered saline (PBS) containing 1% of bovine serum albumin (BSA). The mouse spleen was taken out and minced. RBC Lysis Buffer (00-4300-54, Thermo Fisher Scientific Inc, Waltham, MA, USA) was added to the ground spleen cells. After 5 minutes at room temperature, the lysate was

centrifuged for 5 minutes at 300 g, and the precipitate was resuspended with 200 μL of PBS containing 1% of BSA.

2.4 | Flow cytometry analysis

Splenocytes and peritoneal cells were filtered, and blocked with Fc-blocking solution for 30 minutes. After blocking, all samples received 1 mL of PBS, and were centrifuged at 300 g for 5 minutes: 200 μL of PBS containing 1% of BSA was added to the precipitate for resuspension. Violet stain was used to identify dead cells (L34955, Thermo Fisher Scientific Inc, Waltham, MA, USA). Fluorophore-conjugated antibodies (Ab) (Apc-cy7-CD45, BV510-CD11b, Apc-F4/80, FITC-F4/80, PE-Ly6C, PE-CD11C, Apc-Ly6C, PE-cy7-Ly6G, FITC-Gr-1 (Biolegend, San Diego, CA, USA)) were diluted with PBS containing 1% of BSA. The diluted antibodies were added to the sample tubes. Single positive controls for each diluted antibody were also set up. After incubation at 4°C for 30 minutes in the dark, cells were washed once with PBS and suspended with 100 μL of PBS. Fluorescence data were acquired using Attune NxT flow cytometer (Thermo Fisher Scientific Inc, Waltham, MA, USA) and analyzed by Flowjo Version 10 (Tree Star Inc, Ashland, OR).

2.5 | Preparation of mouse primary bone marrow-derived macrophages (BMDMs)

Macrophages were derived from bone marrow (BM) as done previously.[7] Briefly, male C57BL/6 mice (8 ~ 12 weeks old) were killed by cervical dislocation, and immersed in 75% of ethanol for 5 minutes. Then, the femur and the tibia were cut off, and the muscles and tissues around them were removed with sterile forceps and scissors. The #22 needle of a syringe was inserted into one end of the bone, and the bone marrow cells were flushed out with PBS. After centrifugation at 300 g for 5 minutes, cells were collected and incubated for 7 days with DMEM supplemented with 10% of FBS, 10 ng/mL macrophage-colony stimulating factor (M-CSF) (PeproTech, Rocky Hill, NJ, USA), 1% of penicillin/streptomycin, sodium pyruvate (1 mM) in a humidified 5% of CO_2 incubator at 37°C.

2.6 | Reagents

TP5 of 99.5% purity used in our experiments was produced by Hainan Zhonghe Pharmaceutical Co., Haikou, China. LPS (L6529) from *E coli* O55:B5 was purchased from Sigma-Aldrich (St. Louis, MO, USA). Anti-PPARγ (bsm-33436M) and anti-Phospho-PPARγ (ser273) (bs-4888R) antibodies were purchased from Bioss (Bioss, Wuhan, China). GW9662 (S2915) was purchased from Selleckchem (Selleckchem, Houston, TX, USA).

2.7 | Assays of cytokines, NO, LDH, and 15-d-PGJ2

Concentrations of TNF-α, IL-6, and IL-10 in the plasma or supernatant were determined with commercially available ELISA kits (R & D systems, Minneapolis, MN, USA) according to the manufacturer's instructions. IL-18 and TGF-β ELISA kits were purchased from Dakewe Biotech (Beijing, China). The level of NO in culture media and serum was determined using the Griess reaction (S0021, Beyotime, Nanjing, China). The release of LDH into culture media was determined using LDH assay kit (C0016, Beyotime, Nanjing, China). The level of 15-d-PGJ2 in culture media and serum was determined using an ELISA kit (ADI-900-023, Enzo Life Sciences, Switzerland). The level of PGD2 in culture media was determined using an ELISA kit (512031, Cayman Chemical, Ann Arbor, MI).

2.8 | Total SOD activity

For determination of total SOD activity, the lung samples were homogenized in 1 mol/L HCL. The homogenate was centrifuged at 750 g for 10 minutes. Then, the supernatant was immediately separated and detected by commercial kit (Nanjing Jiancheng Company, China).

2.9 | HE staining

Lung tissues were fixed in 4% of phosphate-buffered formaldehyde solution for more than 24 hours, embedded in paraffin and cut into 4 μm sections. Lung sections were affixed to slides, deparaffinized, and finally, stained with hematoxylin and eosin (H&E). Images were obtained with the Olympus BX41 microscope (Olympus, Japan).

2.10 | Metabolomics

BMDMs were incubated with DMEM (Control) or DMEM containing 100 ng/mL of LPS, 100 ng/mL of TP5, or 100 ng/mL of LPS plus 100 ng/mL of TP5 for 24 hours, washed with ice-cold PBS, digested with 0.25% of trypsin, centrifugated at 300 g for 5 minutes, then, the pellets were washed twice with ice-cold PBS, quenched with 70% of methanol and subjected to three rapid freeze-thaw cycles. The debris was pelleted by centrifugation at 12 000 rpm for 10 minutes at 4°C and the supernatants containing H_2O-soluble metabolites

were collected. Metabolomics was done according to a previous report.[8] Briefly, 2 μL of aliquots of the supernatants were subjected to widely targeted metabolite analysis by Ultra Performance Liquid Chromatography (UPLC) (Waters, Milford, USA) and Tandem mass spectrometry (MS/MS), using a 2.1 mm × 100 mm (1.8 μm) Waters ACQUITY UPLC HSS T3 C18 column (Waters, Milford, USA). The sample manager temperature was held at 4°C and the column oven was set at 40°C. The mobile phase was deionized water containing 0.04% of acetic acid for canal A and acetonitrile containing 0.04% of acetic acid was used for canal B. Flow rate was 0.4 mL/min. A linear gradient for elution was set as follows: 95% A for 0-11 minutes; 5% A for 11-12 minutes; 95% A for 12-12.1 minutes; 95% A for 12.1-14 minutes. By using the positive-ion (ESI^+) and negative-ion (ESI^-) modes, the MS acquisition and MS/MS identification were conducted. The parameters for the MS acquisition were as follow: the MS capillary voltages were set at 5.5 kV in the ESI^+ mode and 4.5 kV in the ESI^- mode. Based on the targeted standards metware database built by Metware Biotech (Wuhan, China), metabolites were identified by their retention times and precursor product ion pair information. The quantity of metabolites were analyzed by multiple reaction monitoring in a Triple quadruple bar mass spectrometer. Data were processed by Analyst 1.6.3 (Agilent, Santa Clara, CA, USA). One QC sample composed of all the 15 samples was run for every 10 samples to ensure the detection stability and replicability of the samples.

2.11 | Metabolomics data analysis

OPLS-DA model was performed by statistical function *prcomp* within R (https://www.r-project.org/). Significantly different metabolites between LPS and LPS plus TP5 were determined by VIP ≥ 1 and absolute Log2FC ≥ 1. VIP values were extracted from OPLS-DA results and generated using R package *ropls*. The identified metabolites were annotated using the KEGG database, and the annotated metabolites were then mapped to the KEGG pathway database. Pathways with significantly different metabolites were then fed into metabolite sets enrichment analysis (MSEA), the significance of which was determined by the *P* values of the hypergeometric test. Violin plots were performed by R package *ggplot2*.

2.12 | Analysis of PGD2 and 15-d-PGJ2 by LC/MS/MS

PGD2 and 15-d-PGJ2 were analyzed by reverse-phase HPLC as done previously.[9] Online HPLC was carried out using a Surveyor MS pump equipped with a Waters ACQUITY-X Bridge BEH C18 (130Å, 1.7 - 3.5 μm, 2.1-4.6 mm × 100-150 mm, 2/pk) at a flow rate of 0.3 mL/min starting with 80% of Phase 1 (water-phase 2-acetic acid, 95:5:0.1) to 30% from 1 to 27.0 minutes and holding at 100% of Phase 2 (acetonitrile-methanol-acetic acid, 95:5:0.1) from 28.0 to 29.0 minutes and returning to 80% of Phase 1 at 30.0 to 32.0 minutes. 15-d-PGJ2 was identified using a Waters ACQUITY UPLC coupled to SYNAPT Q-TOF MS with electrospray ionization (MSE). The mass spectrometer was operated in the negative ion mode. Nitrogen was used as both the sheath gas and the auxiliary gas, at 31 and 17 psi, respectively. The capillary temperature was 300°C. The spray voltage was 3.0 kV, and the tube lens voltage was 80 V. Spectra were displayed by averaging scans across chromatographic peaks. Data-independent acquisition (MSE) was performed according to the characteristic fragmentation patterns of PGD2 and 15-d-PGJ2. The collision energy for MSE was 20 to 50 eV. Data acquisition and analysis were performed using Masslynx 4.1 software (Waters Corporation).

2.13 | Statistical analysis

Statistical analysis in this study was performed using GraphPad Prism 6 (GraphPad Software, Inc). All data represent multiple independent experiments and were represented as mean ± SEM. Statistical significance is calculated using one-way ANOVA corrected with Tukey's multiple comparisons test. Log rank test was applied for survival analysis.

3 | RESULTS

3.1 | TP5 improves survival rate of mice with sepsis

We first explored whether TP5 ameliorated CLP-induced mortality and multiple organ dysfunction. C57BL/6N mice were given s.c. injection of TP5 (10 mg/kg) or NS 0.5 hour after the CLP surgery and on the subsequent 6 days. The survival of mice was monitored for all groups, and the results are shown in Figure 1A. As expected, all mice in the sham group survived. 80% of the mice in vehicle group died within 3 days, and their median survival time was 48 hours. However, almost 65% of the TP5-treated mice survived. As determined by log-rank test, there was a significant difference between the vehicle and TP5 groups. We also took a video of the mice 12 hours after the setup of CLP (Supplementary Video 1). The video showed that TP5-treated mice exhibited less lethargic and tremulous behavior than vehicle-treated mice. Inappropriate hyper-inflammatory and oxidative stress are the hallmarks of sepsis. Therefore, we evaluated the effect of TP5 on inflammation-related cytokines and antioxidant. We observed an upsurge of pro-inflammatory cytokines including IL-6 and TNF-α and chemokine CCL2 after 24 hours of CLP surgery, all of them were markedly decreased by TP5 treatment (Figure 1B-D). As previously reported, sepsis induced an increase of NO and diminished

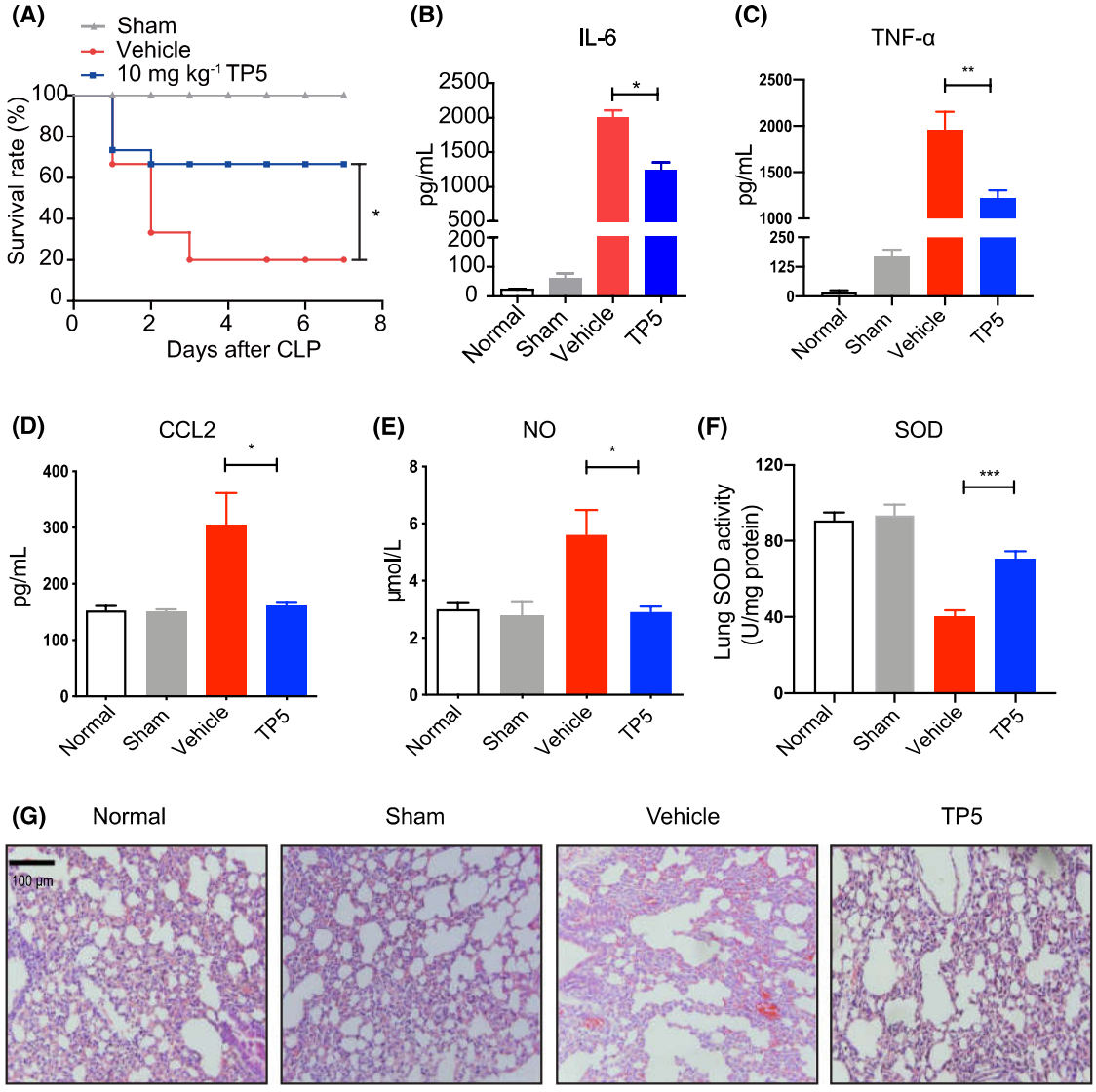

FIGURE 1 Functional effect of TP5 on CLP induced sepsis. A, Mortality after TP5 (10 mg/kg) was injected s.c. 0.5 hour after CLP in C57BL/6N mice. Animals were monitored for 7 d after CLP (n = 15). B-E, C57BL/6N mice were subjected to CLP, and then, given TP5 or sham operated (n = 5). Experiments were terminated 24 hours after CLP, and blood was collected for analysis. Inflammatory mediators IL-6 (B), TNF-α (C), CCL2 (D), and NO (E) were determined in plasma. F, Total SOD activity in the lung tissues 24 hours after CLP of all groups were detected by commercial kit (n = 5). G, Photomicrographs of representative HE-stained lungs obtained after 24 hours CLP-induced sepsis shown. Scale bar 100 μm. Data are expressed as mean ± SEM. *$P < .05$, **$P < .01$, ***$P < .001$

the activity of SOD,[10,11] while TP5 reversed the increased production of NO and decreased activity of SOD almost back to normal (Figure 1E,F). Furthermore, pathological analysis revealed that TP5 administration visibly reduced the amount of inflammatory infiltrate and hyperemia (Figure 1G). These results suggest that TP5 may potently protect mice from the effects of sepsis.

3.2 | TP5 diminishes the infiltration of macrophage and granulocyte in the peritoneal cavity and spleen

As macrophage and granulocyte play an essential role in early stage of sepsis,[12] we set out to detect the influx of them in the peritoneal cavity and spleen. As it was shown in Figure 2A, both Sham and CLP operation induced a disappearance of $CD11b^{low}F4/80^{high}$ subset and an increase of $CD11b^{high}F4/80^{low}$ subset, which also called large peritoneal macrophages (LPMs) and small peritoneal macrophages (SPMs), respectively.[13] LPMs were demonstrated to migration to the omentum upon infections.[14] SPMs express higher levels of MHC-II, TLR4, TNF-α, IL-1β, IL-12, NO, and IL-1α after infections, indicating that SPMs tend to be M1-like macrophage.[15,16] We observed that TP5 treatment decreased the proportion of SPMs but not alter the disappearance of LPMs. As SPMs are generated from bone-marrow-derived myeloid precursors, we further analyzed the composition of SPMs by Ly6C expression. Results showed that there was a markedly

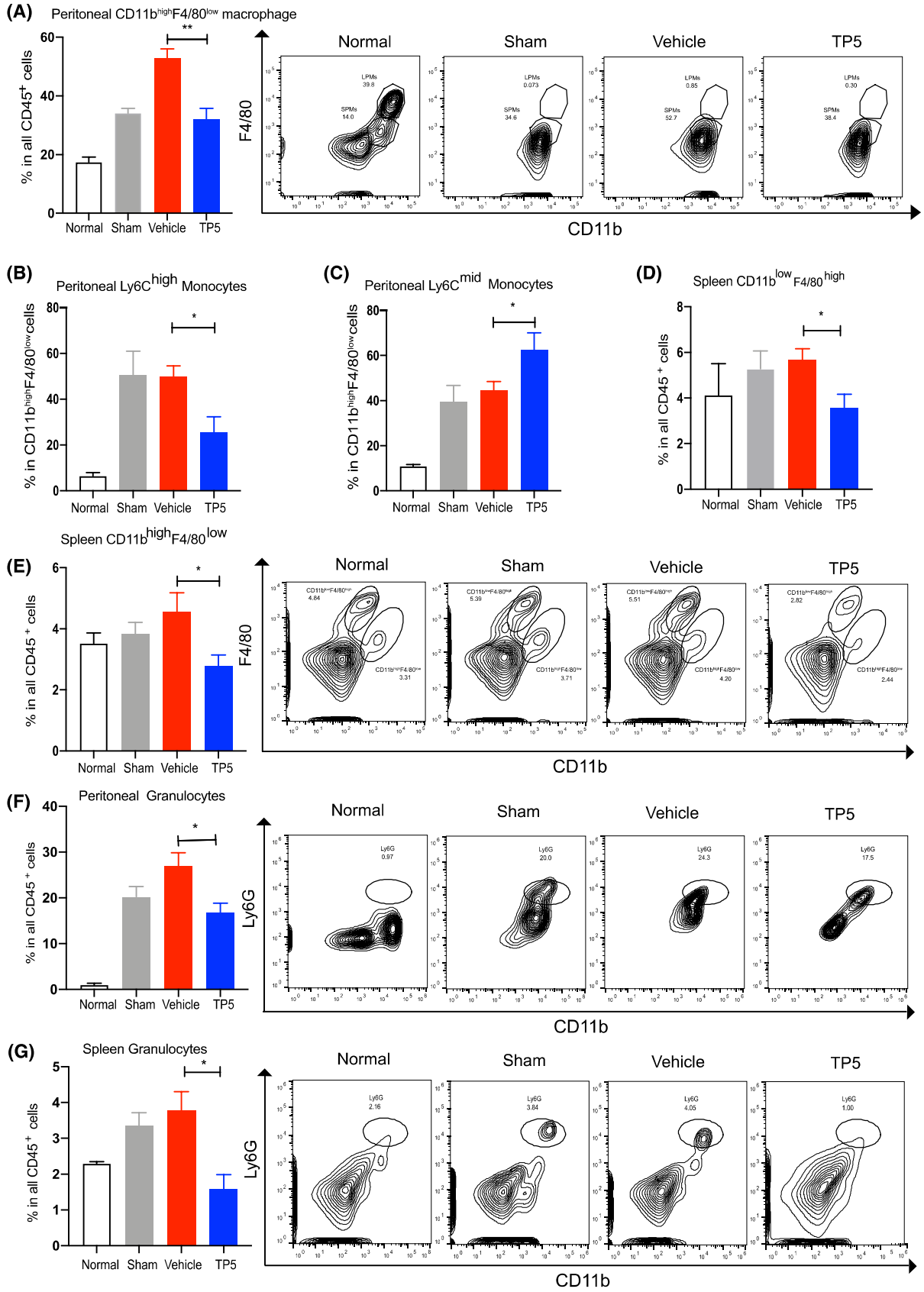

FIGURE 2 The proportion of macrophage and granulocyte subsets in the peritoneal cavity and spleen were analyzed 12 hours after CLP by FACS (n = 5). A, Percentage and representative images of $CD11b^{high}F4/80^{low}$ subset in the peritoneal cavity. B-C, Percentage of $CD11b^{high}F4/80^{low}Ly6C^{high}$ and $CD11b^{high}F4/80^{low}Ly6C^{mid}$ subsets in $CD11b^{high}F4/80^{low}$ macrophage. D-E, Percentage and representative images of $CD11b^{low}F4/80^{high}$ and $CD11b^{high}F4/80^{low}$ subsets in the spleen. F-G, Percentage and representative images of $CD11b^{+}Ly6G^{+}$ subsets in the peritoneal cavity and spleen. Data are expressed as mean ± SEM. $^{*}P < .05$

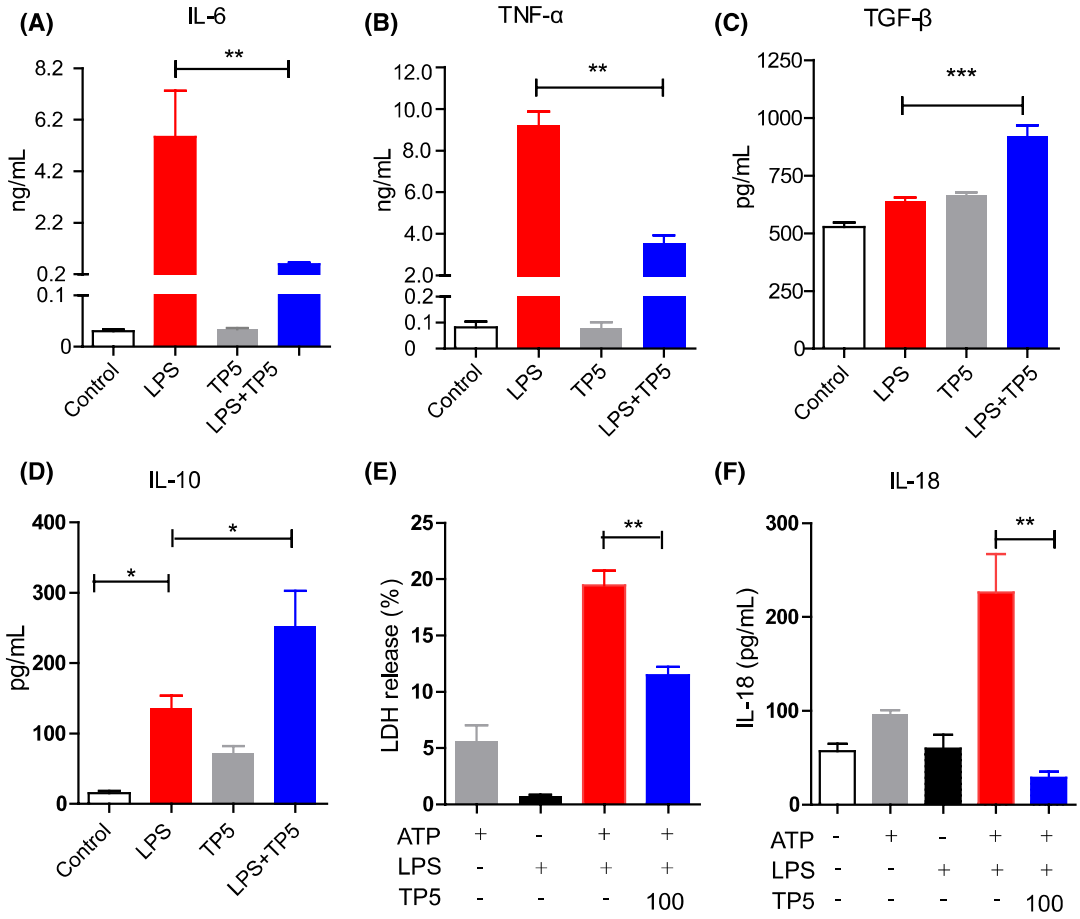

FIGURE 3 TP5 treatment reduces pro-inflammatory cytokines release from BMDMs upon LPS stimulation in vitro. A and B, BMDMs were treated with medium (DMEM), LPS (100 ng/mL), TP5 (100 ng/mL), and LPS plus TP5 for 24 hours. Release of IL-6 (A) and TNF-α (B) was measured (n = 3). C and D, Concentrations of anti-inflammatory cytokine TGF-β (C) and IL-10 (D) in BMDMs treated with LPS and TP5 were determined using ELISA (n = 3). E and F, BMDMs were primed with LPS for 4 hours in the presence or absence of TP5, followed by the addition of ATP for 0.5 hour. LDH and IL-18 release into the supernatant was determined (n = 3). Data are expressed as mean ± SEM. $*P < .05$, $**P < .01$, $***P < .001$

increase of Ly6C^{high} and Ly6C^{mid} monocytes in Sham and CLP groups, while TP5 treatment reversed this effect by inhibiting the upsurge of Ly6C^{high} monocytes but increasing the percentage of the Ly6C^{mid} monocytes (Figure 2B,C). We also analyzed the composition of macrophage subsets in spleen. We observed that Sham and CLP groups tended to have an increase of different subsets of macrophage, although not significant, while TP5 administration decreased the percentage of CD11b^{low}F4/80^{high} and CD11b^{high}F4/80^{low} subsets in the spleen (Figure 2D,E), which represented red pulp and marginal zone macrophage, respectively.[17] Red pulp macrophages are distinguished with CD11b^{low}, F4/80^{high}, CD163, and SIRPα expression and thought to be M1-like macrophage upon infections as they own the enhanced ability to accumulate iron.[18] Marginal metallophilic macrophages and marginal zone macrophages also display M1-like phenotype after infection in the early stage as they are the major producers of IFN-γ and express higher level of LT, TNF-α.[19] Furthermore, the migration of granulocytes to the peritoneum and spleen was also inhibited (Figure 2F,G). The data from these observations emphasize that TP5 diminishes the infiltration of macrophage and granulocyte which may contribute to its protective effect on sepsis.

3.3 | TP5 inhibits pro-inflammatory cytokines release in LPS-stimulated macrophages

Given the well-known function of macrophages in the pathogenesis of sepsis,[20] we first investigated the effect of TP5 in LPS-stimulated BMDMs. We observed that a 100 ng/mL of LPS stimulation for 24 hours induced a robust increase of TNF-α and IL-6 release. These increases were significantly suppressed by TP5 (Figure 3A,B). In addition, BMDMs treated with TP5 showed higher releases of anti-inflammatory cytokines, including TGF-β and IL-10 (Figure 3C,D). Inflammasome activation has been reported to be a central event in the pathogenesis of sepsis, which robustly increases the level of IL-18 and IL-1β and damages mitochondria,

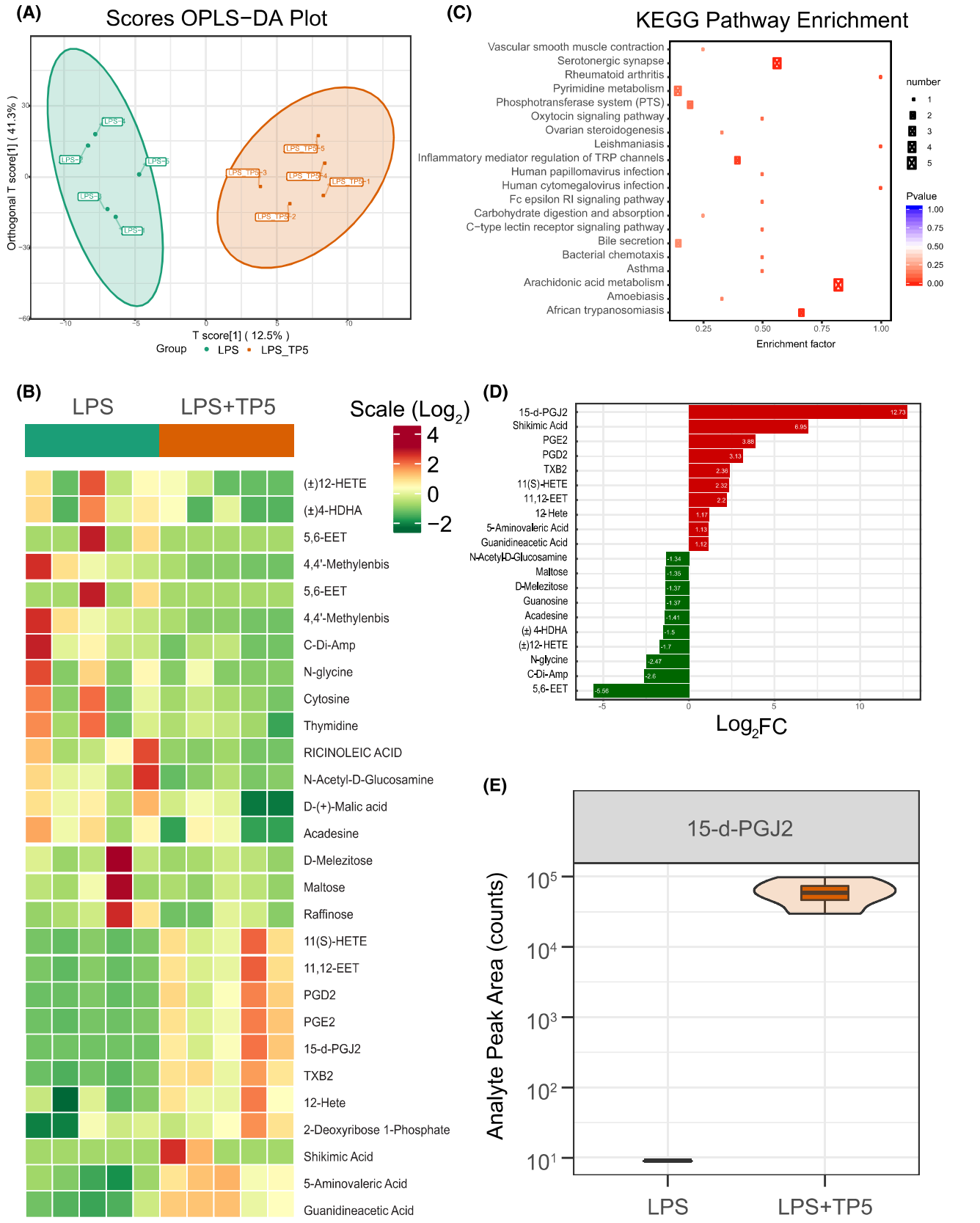

FIGURE 4 Metabolomic analysis of different metabolites and enriched pathways in LPS-primed BMDMs with or without TP5. A, Principal-component analysis (PCA) plot of metabolites in LPS-primed BMDMs with or without TP5 (n = 5). B, Hierarchical clustering of differential metabolites between the above-mentioned two groups. C, Statistics of KEGG pathway enrichment in the above-mentioned two groups (red, upregulated; blue, downregulated). D, Fold change of differential metabolites in LPS plus TP5-treated BMDMs compared to LPS-stimulated BMDMs. (E) Violin plot of 15-d-PGJ2 metabolites synthetized by BMDMs (n = 5)

leading to abnormal alterations of multiple organs.[21,22] Thus, we determined the effect of TP5 on inflammasome activation by LPS and ATP in stimulated macrophages. The results showed TP5 treatment substantially decreased the release of LDH into the supernatant (Figure 3E), and also the secretion of IL-18 (Figure 3F). Together, these results indicate that TP5 has an inhibitory effect on pro-inflammatory cytokines release in LPS-stimulated macrophages.

3.4 | TP5 alters the metabolomics of LPS-stimulated macrophages

Upon infection, it is known that innate immune cells increase their metabolic throughput, promoting energy generation and biosynthesis.[23] In addition, there is a direct link between metabolic intermediates and regulation of epigenetic landscapes.[24] Recently metabolomics have been widely used to identify biomarkers associated with the onset and progression of sepsis.[25] Thus, we conducted a widely targeted LC-MS/MS-based metabolome detection assay in both LPS only and LPS plus TP5-treated macrophages ($n = 5$). Principal-component analysis (PCA) segregated the metabolome profile of LPS plus TP5 from LPS-stimulated macrophages (Figure 4A). Figure 4B shows different metabolites between the two groups which were selected by fold change ≥ 2 or fold change ≤ 0.5 and Variable Importance in Projection (VIP) ≥ 1, an important score based on orthogonal partial least squares-discriminant analysis (OPLS-DA) plots.[26] Furthermore, the Kyoto Encyclopedia of Genes and Genomes (KEGG) pathway analysis associated with different metabolites exhibited a remarkable enrichment of arachidonic acid (AA) metabolism between the two groups (Figure 4C). Five of six metabolites in the AA metabolism pathway were increased in the LPS plus TP5 group compared to the LPS group. 15-d-PGJ2 was the most significantly different metabolite in the analyzed metabolomes (Figure 4D). The robust increase of 15-d-PGJ2 upon TP5 treatment is depicted in Figure 4E. The significantly different metabolites are listed in Supplementary Table 1. Based on the metabolic profiling results, we can infer that significant changes, related to arachidonic acid (AA) metabolism, occurred in TP5-treated macrophages primed with LPS.

3.5 | TP5 promotes the production of PGD2 and 15-d-PGJ2

To validate the increase of 15-d-PGJ2 levels in vivo, we collected the plasma from CLP-induced septic mice and examined the level of 15-d-PGJ2 by ELISA. As shown in Figure 5A, there was no significant difference between CLP-induced septic and sham operated mice as well as control mice, whereas TP5 treatment markedly boosted the production of 15-d-PGJ2 with an accompanying increase of TGF-β (Figure 5B). We also determined the level of 15-d-PGJ2 in the supernatant from macrophages subjected to different treatments. In agreement with the in vivo results, there was a dramatic increase of 15-d-PGJ2 in both the TP5 and LPS plus TP5-treated groups (Figure 5C). We next tested whether the production of 15-d-PGJ2 was increased by TPS in a dose dependent manner. We, thus, treated macrophages with 0, 10, 50, and 100 ng/mL of TP5 for 48 hours. The result showed that the production of 15-d-PGJ2 was increased in a concentration-dependent manner (Figure 5D). Furthermore, to clarify whether the production of 15-d-PGJ2 depended on single amino acids or whole TP5, we synthetized tetrapeptide (Lys-Asp-Val-Tyr), tripeptide (Asp-Val-Tyr), dipeptide (Val-Tyr), and treated BMDMs with 0.15 μM (≈100 ng/mL) TP5, tetrapeptide, tripeptide, dipeptide, and the amino acid arginine for 48 hours. Then, the supernatant was collected for the determination of 15-d-PGJ2. The result showed that synthetic peptides without arginine could not promote the production of 15-d-PGJ2. Interestingly, arginine alone partly mimicked the function of TP5 (Figure 5E). To dissect the underlying mechanisms causing the increase in 15-d-PGJ2, we examined the level of PGD2, which is the precursor of 15-d-PGJ2. First, we analyzed the data from metabolite analysis and found that TP5 considerably promoted the production of PGD2 in LPS-stimulated macrophages (Figure 5F). Subsequently, we confirmed this result by ELISA. Consistent with the metabolomics result, the addition of TP5 increased the production of PGD2 (Figure 5G). Second, to confirm whether TP5 catalyzed the metabolism of PGD2 to 15-d-PGJ2, we incubated PGD2 with PBS or 100 ng/mL of TP5 at 37°C for 24 hours and analyzed the products by LC-MS-MS. The result showed that there were almost equal PGD2, 15-d-PGJ2 and other byproducts in both groups (Supplementary Figure 1A-E), indicating that TP5 has no effect on the dehydration process. Thus, our results indicate that TP5 may effectively promote the production of PGD2 and 15-d-PGJ2.

3.6 | The activation of PPARγ mediates the protective effect of TP5

15-d-PGJ2 is a dehydration product of PGD2 and has a highly reactive cyclopentenone ring, which readily reacts with substances containing nucleophilic groups and covalently modifies proteins.[27,28] It has been reported that 15-d-PGJ2 exerts an anti-inflammatory effect by binding to PPARγ.[29,30] Therefore, we examined the phosphorylation of PPARγ with or without TP5 treatment in LPS-stimulated macrophages. The pretreatment with TP5 induced an increase in the phosphorylation of PPARγ (ser273), which is essential for the function of PPARγ, without altering the total level of PPARγ (Figure 6A,B). We

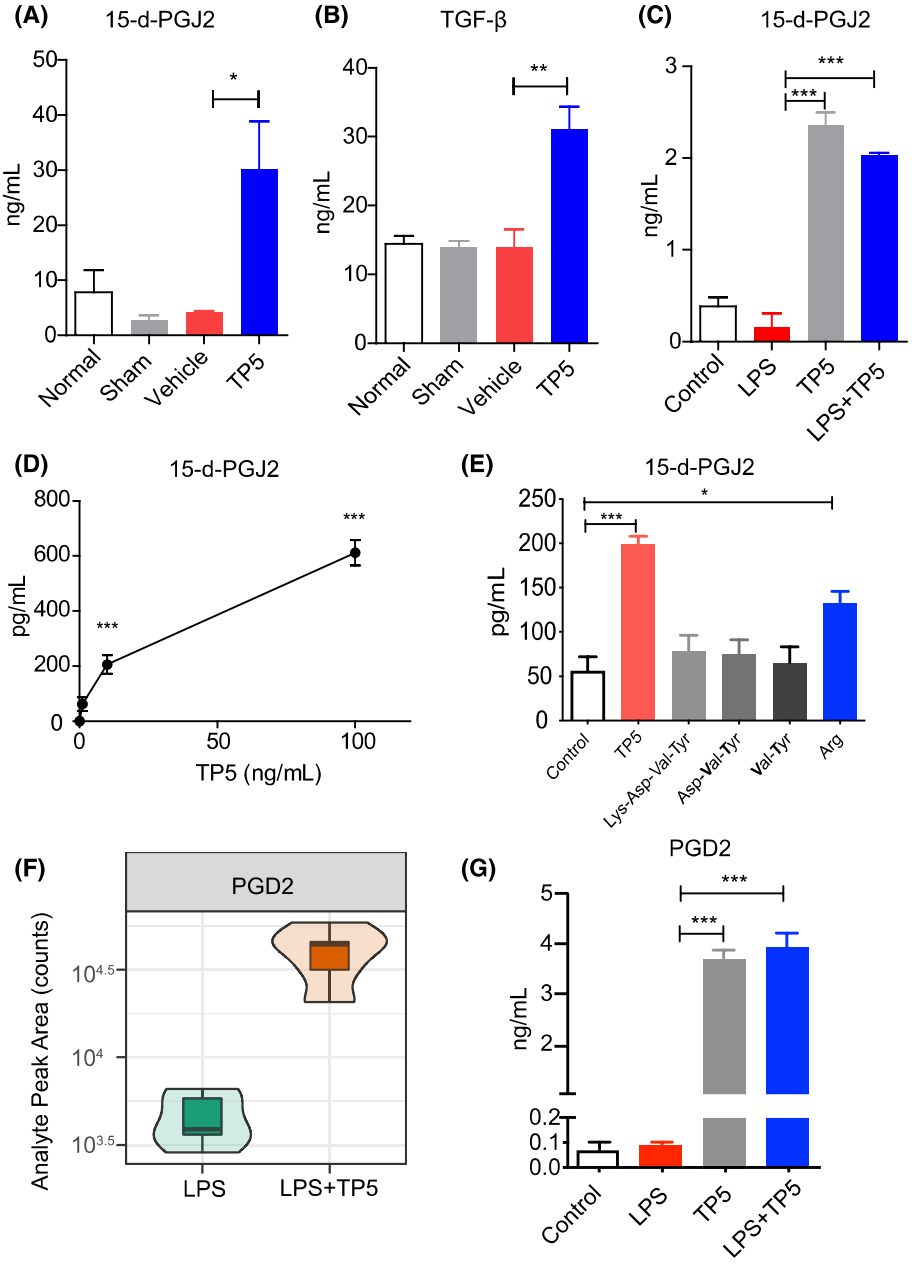

FIGURE 5 TP5 promotes the production of 15-d-PGJ2 in vitro and in vivo. A and B, Mice were injected s.c. with NS or 10 mg/kg TP5 0.5 hour after CLP. The plasma was collected 12 hours after CLP. Plasma 15-d-PGJ2 (A) and TGF-β (B) levels were measured by ELISA (n = 5). C, Release of 15-d-PGJ2 from BMDMs was measured 48 hours after in vitro LPS (n = 5). D, BMDMs were treated with 0, 1, 10, 100 ng/mL TP5 for 48 hours, the level of 15-d-PGJ2 in the supernatant was determined (n = 5). E, BMDMs were treated with 0.15 μM each of TP5, tetrapeptide (Lys-Asp-Val-Tyr), tripeptide (Lys-Asp-Val), dipeptide (Lys-Asp), and arginine for 48 hours. The level of 15-d-PGJ2 was determined (n = 5). F, Violin plot of PGD2 metabolites in BMDMs lysates with LPS or LPS plus TP5 treatment for 48 hours (n = 5). G, Release of PGD2 was measured 48 hours after LPS stimulation of BMDMs with or without TP5 treatment (n = 5). Data are expressed as mean ± SEM. *$P < .05$, **$P < .01$, ***$P < .001$

next assessed whether TP5's improvement of sepsis depended on PPARγ activation in vitro and in vivo. GW9662 is an irreversible and selective PPARγ antagonist that can modify a cysteine residue in the ligand-binding site of PPARγ.[31] GW9662 was used at a concentration that did not affect cellular viability. The result showed that GW9662 treatment considerably increased TNF-α and IL-6 levels (Figure 6C,D). Likewise, GW9662 also inhibited the anti-inflammatory effect of TP5, as shown by the decreased production of TGF-β (Figure 6E). Moreover, GW9662 counteracted the protective effect of TP5 against sepsis. As depicted in Figure 6F, the TP5-prolonged survival after CLP was reversed by GW9662. These data indicate that the anti-sepsis effect of TP5 relies on PPARγ activation. Together, our results suggest that TP5 promotes the production of 15-d-PGJ2 and modulates the activation of PPARγ in macrophages.

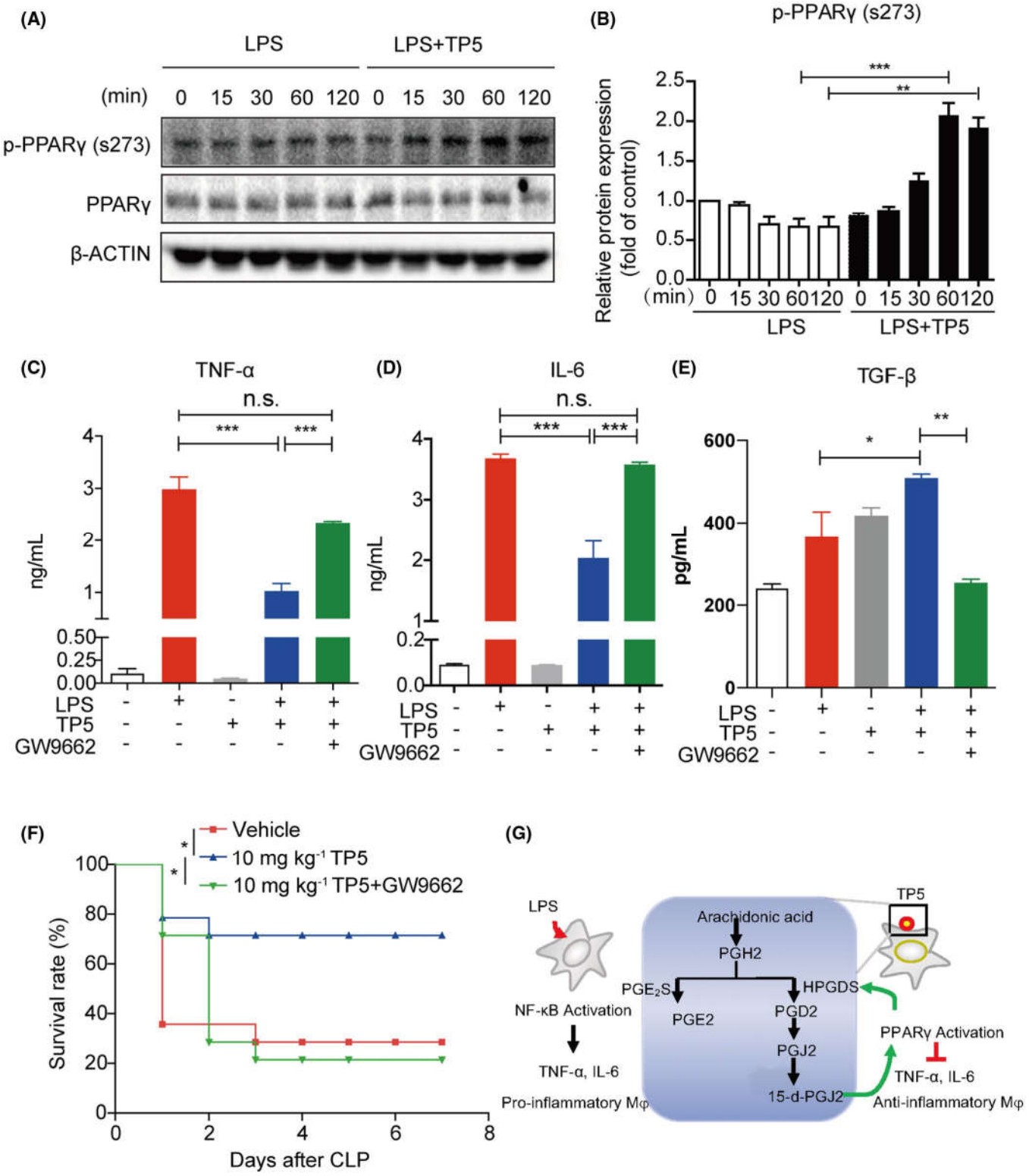

FIGURE 6 TP5 improves the survival of CLP-induced sepsis in a PPARγ-dependent manner. A, Representative Western blot of protein expression in BMDMs treated with LPS or LPS plus TP5 for the indicated times (n = 3). B, Quantitative analysis of the protein level of p-PPARγ (s273). C-E, Concentrations of TNF-α, IL-6, and TGF-β were measured in the supernatant of BMDMs treated with LPS and TP5 with or without GW9662 (10 μM) for 48 hours (n = 3). F, Survival of mice subjected to CLP treated with NS, TP5, and TP5 plus GW9662 (1 mg/kg/day) (n = 14 per group). G, Graphical abstract illustrating the therapeutic effect of TP5 on sepsis. TP5. Data are expressed as mean ± SEM. $^{*}P < .05$, $^{**}P < .01$, $^{***}P < .001$

4 | DISCUSSION

Activation of the innate immune system is essential to protect the host from infection, but this activation must be tightly regulated, because excessive inflammation will contribute to the pathogenesis of multiple organ failure that may result in septic shock, the most severe form of sepsis with an increased mortality.[12] Thus, resolution of inflammation by eliminating pro-inflammatory cytokines or releasing the anti-inflammatory mediators is essential to maintain homeostasis and may exert protection in sepsis. This study used TP5 to combat sepsis, and found that TP5 made a profound improvement in the damage caused by CLP-induced sepsis.

To determine the underlying molecular mechanisms of the protective effect of TP5 on sepsis, we focused on the regulation of macrophage infiltration and polarization, which is an essential participant in both the amplification of inflammation at onset of injury and downregulation of the inflammatory response by tissue repairing.[32] These divergent roles of macrophages depend on environmental cues, which promote a spectrum of macrophage phenotypes ranging from M1 pro-inflammatory to M2 anti-inflammatory. The M1 phenotype, induced by LPS and IFN-γ, is characterized by the expression of pro-inflammatory cytokines including TNF-α, IL-6, and IL-1β, promotion of T helper 1 response, and tissue injury. M2 macrophages induced by IL-4 or IL-13, however, exert mainly anti-inflammatory functions, and are involved in tissue repair.[33] In our experiments, stimulation with LPS (100 ng/mL) for 24 hours led to significant increases in IL-6, TNF-α, and IL-10, but not TGF-β in macrophages. TP5 effectively inhibited the level of inflammatory monocytes chemokine CCL2 and pro-inflammatory cytokines IL-6 and TNF-α. Moreover, the presence of TP5 increased the anti-inflammatory cytokines TGF-β and IL-10, and TP5 treatment suppressed the activation of NLRP3 inflammasomes, which were recognized as culprits in the sepsis.[34] These results suggest TP5 displays a great anti-inflammatory potency by promoting M2 polarization.

Recent studies have demonstrated that regulation of immunometabolism may be a new therapy for sepsis.[35,36] Danger-associated molecule patterns (DAMPs) or Pathogen-associated molecule patterns (PAMPs) stimulate cellular responses mediated by pattern-recognition receptors (PRRs), resulting in a disorder of immunometabolism.[2] It is well known that LPS-treated macrophages cause the activation of phospholipase A2 (PLA2), which catalyzes hydrolytic release of AA from membrane phospholipids.[37] Then, cyclooxygenases (COX-1 and COX-2) and 15-lipoxygenase (15-LOX) catalyze oxidative conversion of AA to prostaglandin H2 (PGH2) and 15S-hydroperoxy-5Z, 8Z, 11Z, and 13E-eicosatetraenoic acid (15-HpETE), respectively. Subsequently, hematopoietic prostaglandin D synthase (HPGDS) metabolizes PGH2 to PGD2 conversion. PGD2 undergoes chemical dehydration, losing water to form the cyclopentenone prostaglandin PGJ2. Finally, PGJ2 undergoes further conversion to 12-d-PGJ2 and 15-d-PGJ2 by losing one hydroxyl and two hydroxyl groups, respectively.[38] In our study, we found AA metabolism signatures in the LPS plus TP5-treated macrophage lysates compared with LPS-stimulated macrophage lysates. The drastic increase of 15-d-PGJ2, PGE2, and PGD2 contributed to the enrichment of AA metabolism, especially the generation of metabolites of 15-d-PGJ2 and PGD2. Both PGD2 and 15-d-PGJ2 have anti-inflammatory effects, however, PGD2 is inherently not stable in physiologic solutions as albumin catalyzes the dehydration of PGD2 to 15-d-PGJ2.[9,27] Thus, 15-d-PGJ2 maybe a major contributor to the improved survival to sepsis upon TP5 treatment. As AA metabolism presents almost all cells,[39] it is noteworthy that TP5 may not only regulate the function of immune cells, but also AA abundant cells such as adipocytes, endothelial cells and hepatocytes. Besides, since AA is a major component of cell membrane, TP5 may act on the cell membrane directly without transporter. As HPGDS is a rate limiting enzyme for the production of 15-d-PGJ2, we are working on whether HPGDS is a target for TP5.

15-d-PGJ2 is a cyclopentenone PG (cyPG) containing an α,β-unsaturated ketone, which turns 15-d-PGJ2 more electrophilic and reactive. It has been reported that 15-d-PGJ2 can bind to cysteine residue in the PPARγ ligand binding domain through a Michael addition.[29,40] PPARγ has long been known as an anti-inflammatory transcription factor, as well as an inhibitor of the activation of the NLRP3 inflammasome.[41,42] 15-d-PGJ2 is known to act on multiple tissues to improve organ failure by reducing pro-inflammatory cytokines.[43-46] Therefore, the increase of 15-d-PGJ2 may explain its obvious effect in the decrease pro-inflammatory cytokines, as well as the increased anti-inflammatory cytokines.

We have demonstrated that TP5 protects against sepsis by producing 15-d-PGJ2 and activating the PPARγ signaling pathway. It has been reported that PPARγ could increase the expression of HPGDS via transcriptional regulation.[47] Thus, in TP5 treated macrophages, the upregulation HPGDS leads to the enhanced production of 15-d-PGJ2, which not only acts in a positive feedback loop to promote the transcription of HPGDS, but also increases the anti-inflammatory cytokine expression, including TGF-β and IL-10. Taken together, our result strongly supports the possibility of a feed-forward loop involving the HPGDS - 15-d-PGJ2 - PPARγ - HPGDS as depicted in Figure 6G.

Therefore, our study demonstrates that TP5 exhibits a number of pharmacological effects in septic mice by shunting the AA metabolism toward the production of 15-d-PGJ2 and could be an effective drug candidate.

ACKNOWLEDGMENT

We kindly express our appreciation to Hui Ye (Public platform of State Key Laboratory of Natural Medicines) for her assistance of LC-MS/MS detection. This work was supported by the National Natural Science Foundation of China (Nos 81703562, 81571984 and 81703563), the Jiangsu Province Natural Science Foundation of China (No BK20170732), and 'Double First-Class' University project (No CPU2018GF10 and CPU2018GY46).

CONFLICT OF INTEREST

The authors declare that they have no conflict of interests regarding the publication of this paper.

AUTHOR CONTRIBUTIONS

X. Li and D. Qin designed the experiments; Y. Zhang, X. Yang, R. Li, Q. Y, and L. You performed the experiments; X. Li and D. Qin wrote the manuscript; W. Yan helped with the LC-MS/MS data analysis; W. Xie, K. Mo, R. Fu, Y. Wang, Y. Chen, and H. Hou helped with the animal experiment; Y. Yang and L. Birnbaumer supervised and provided critical suggestions throughout the study, and revised the manuscript.

REFERENCES

1. van der Poll T, van de Veerdonk FL, Scicluna BP, Netea MG. The immunopathology of sepsis and potential therapeutic targets. *Nat Rev Immunol*. 2017;17:407-420.
2. Deutschman CS, Tracey KJ. Sepsis: current dogma and new perspectives. *Immunity*. 2014;40:463-475.
3. O'Neill LA, Kishton RJ, Rathmell J. A guide to immunometabolism for immunologists. *Nat Rev Immunol*. 2016;16:553-565.
4. Singh VK, Biswas S, Mathur KB, Haq W, Garg SK, Agarwal SS. Thymopentin and splenopentin as immunomodulators. *Current status. Immunol Res*. 1998;17:345-368.
5. Fan YZ, Chang H, Yu Y, et al. Thymopentin (TP5), an immunomodulatory peptide, suppresses proliferation and induces differentiation in HL-60 cells. *Biochim Biophys Acta*. 2006;1763:1059-1066.
6. Rittirsch D, Huber-Lang MS, Flierl MA, Ward PA. Immunodesign of experimental sepsis by cecal ligation and puncture. *Nat Protoc*. 2009;4:31-36.
7. Li X, Wang D, Chen Z, et al. Galphai1 and Galphai3 regulate macrophage polarization by forming a complex containing CD14 and Gab1. *Proc Natl Acad Sci USA*. 2015;112:4731-4736.
8. Chen W, Gong L, Guo Z, et al. A novel integrated method for large-scale detection, identification, and quantification of widely targeted metabolites: application in the study of rice metabolomics. *Mol Plant*. 2013;6:1769-1780.
9. Cao H, Xiao L, Park G, et al. An improved LC-MS/MS method for the quantification of prostaglandins E(2) and D(2) production in biological fluids. *Anal Biochem*. 2008;372:41-51.
10. Hickey MJ, Sharkey KA, Sihota EG, et al. Inducible nitric oxide synthase-deficient mice have enhanced leukocyte-endothelium interactions in endotoxemia. *FASEB J*. 1997;11:955-964.
11. Fujimura N, Sumita S, Aimono M, et al. Effect of free radical scavengers on diaphragmatic contractility in septic peritonitis. *Am J Respir Crit Care Med*. 2000;162:2159-2165.
12. Hotchkiss RS, Monneret G, Payen D. Sepsis-induced immunosuppression: from cellular dysfunctions to immunotherapy. *Nat Rev Immunol*. 2013;13:862-874.
13. Ghosn EE, Cassado AA, Govoni GR, et al. Two physically, functionally, and developmentally distinct peritoneal macrophage subsets. *Proc Natl Acad Sci USA*. 2010;107:2568-2573.
14. Okabe Y, Medzhitov R. Tissue-specific signals control reversible program of localization and functional polarization of macrophages. *Cell*. 2014;157:832-844.
15. Cassado Ados A, D'Imperio Lima MR, Bortoluci KR. Revisiting mouse peritoneal macrophages: heterogeneity, development, and function. *Front Immunol*. 2015;6:225.
16. Dioszeghy V, Rosas M, Maskrey BH, et al. 12/15-Lipoxygenase regulates the inflammatory response to bacterial products in vivo. *J Immunol*. 2008;181:6514-6524.
17. A-Gonzalez N, Castrillo A. Origin and specialization of splenic macrophages. *Cell Immunol*. 2018;330:151-158.
18. Borges da Silva H, Fonseca R, Pereira RM, Cassado Ados A, Alvarez JM, D'Imperio Lima MR. Splenic macrophage subsets and their function during blood-borne infections. *Front Immunol*. 2015;6:480.
19. Eloranta ML, Alm GV. Splenic marginal metallophilic macrophages and marginal zone macrophages are the major interferon-alpha/beta producers in mice upon intravenous challenge with herpes simplex virus. *Scand J Immunol*. 1999;49:391-394.
20. Kim SJ, Baek KS, Park HJ, Jung YH, Lee SM. Compound 9a, a novel synthetic histone deacetylase inhibitor, protects against septic injury in mice by suppressing MAPK signalling. *Br J Pharmacol*. 2016;173:1045-1057.
21. Ward PA, Fattahi F. New strategies for treatment of infectious sepsis. *J Leukoc Biol*. 2019;106:187-192.
22. Pfalzgraff A, Weindl G. Intracellular lipopolysaccharide sensing as a potential therapeutic target for sepsis. *Trends Pharmacol Sci*. 2019;40:187-197.
23. Phan AT, Goldrath AW, Glass CK. Metabolic and epigenetic coordination of T cell and macrophage immunity. *Immunity*. 2017;46:714-729.
24. Li X, Egervari G, Wang Y, Berger SL, Lu Z. Regulation of chromatin and gene expression by metabolic enzymes and metabolites. *Nat Rev Mol Cell Biol*. 2018;19:563-578.
25. Mills EL, Ryan DG, Prag HA, et al. Itaconate is an anti-inflammatory metabolite that activates Nrf2 via alkylation of KEAP1. *Nature*. 2018;556:113-117.
26. Thevenot EA, Roux A, Xu Y, Ezan E, Junot C. Analysis of the human adult urinary metabolome variations with age, body mass index, and gender by implementing a comprehensive workflow for univariate and OPLS statistical analyses. *J Proteome Res*. 2015;14:3322-3335.
27. Fitzpatrick FA, Wynalda MA. Albumin-catalyzed metabolism of prostaglandin D2. Identification of products formed in vitro. *J Biol Chem*. 1983;258:11713-11718.
28. Bell-Parikh LC, Ide T, Lawson JA, McNamara P, Reilly M, FitzGerald GA. Biosynthesis of 15-deoxy-delta12,14-PGJ2 and the ligation of PPARgamma. *J Clin Invest*. 2003;112:945-955.
29. Shiraki T, Kamiya N, Shiki S, Kodama TS, Kakizuka A, Jingami H. Alpha, beta-unsaturated ketone is a core moiety of natural

ligands for covalent binding to peroxisome proliferator-activated receptor gamma. *J Biol Chem*. 2005;280:14145-14153.
30. Kansanen E, Kivela AM, Levonen AL. Regulation of Nrf2-dependent gene expression by 15-deoxy-Delta 12,14-prostaglandin J2. *Free Radic Biol Med*. 2009;47:1310-1317.
31. Tsukahara T. The role of PPARgamma in the transcriptional control by agonists and antagonists. *PPAR Res*. 2012;2012:362361.
32. Wynn TA, Chawla A, Pollard JW. Macrophage biology in development, homeostasis and disease. *Nature*. 2013;496:445-455.
33. Liu YC, Zou XB, Chai YF, Yao YM. Macrophage polarization in inflammatory diseases. *Int J Biol Sci*. 2014;10:520-529.
34. Kalbitz M, Fattahi F, Grailer JJ, et al. Complement-induced activation of the cardiac NLRP3 inflammasome in sepsis. *FASEB J*. 2016;30:3997-4006.
35. Cheng SC, Scicluna BP, Arts RJ, et al. Broad defects in the energy metabolism of leukocytes underlie immunoparalysis in sepsis. *Nat Immunol*. 2016;17:406-413.
36. McCall CE, Zabalawi M, Liu T, et al. Pyruvate dehydrogenase complex stimulation promotes immunometabolic homeostasis and sepsis survival. *JCI Insight*. 2018;3. https://doi.org/10.1172/jci.insight.99292.
37. Baek SH, Kwon TK, Lim JH, et al. Secretory phospholipase A2-potentiated inducible nitric oxide synthase expression by macrophages requires NF-kappa B activation. *J Immunol*. 2000;164:6359-6365.
38. Harmon GS, Lam MT, Glass CK. PPARs and lipid ligands in inflammation and metabolism. *Chem Rev*. 2011;111:6321-6340.
39. Serhan CN. Treating inflammation and infection in the 21st century: new hints from decoding resolution mediators and mechanisms. *FASEB J*. 2017;31:1273-1288.
40. Powell WS. 15-Deoxy-delta12,14-PGJ2: endogenous PPARgamma ligand or minor eicosanoid degradation product? *J Clin Invest*. 2003;112:828-830.
41. Nelson VL, Nguyen HCB, Garcia-Canaveras JC, et al. PPARgamma is a nexus controlling alternative activation of macrophages via glutamine metabolism. *Genes Dev*. 2018;32:1035-1044.
42. Liu X, Wang Y, Wu D, et al. Magnolol prevents acute alcoholic liver damage by activating PI3K/Nrf2/PPARgamma and inhibiting NLRP3 signaling pathway. *Front Pharmacol*. 2019;10:1459.
43. Collin M, Patel NS, Dugo L, Thiemermann C. Role of peroxisome proliferator-activated receptor-gamma in the protection afforded by 15-deoxydelta12,14 prostaglandin J2 against the multiple organ failure caused by endotoxin. *Crit Care Med*. 2004;32:826-831.
44. Chen K, Li J, Wang J, et al. 15-deoxy- gamma 12,14-prostaglandin J2 reduces liver impairment in a model of ConA-induced acute hepatic inflammation by activation of PPAR gamma and reduction in NF- kappa B activity. *PPAR Res*. 2014;2014:215631.
45. Cuzzocrea S, Pisano B, Dugo L, et al. Rosiglitazone and 15-deoxy-delta 12,14-prostaglandin J2, ligands of the peroxisome proliferator-activated receptor-gamma (PPAR-gamma), reduce ischaemia/reperfusion injury of the gut. *Br J Pharmacol*. 2003;140:366-376.
46. Cuzzocrea S, Ianaro A, Wayman NS, et al. The cyclopentenone prostaglandin 15-deoxy-delta(12,14)- PGJ2 attenuates the development of colon injury caused by dinitrobenzene sulphonic acid in the rat. *Br J Pharmacol*. 2003;138:678-688.
47. Gandhi UH, Kaushal N, Ravindra KC, et al. Selenoprotein-dependent up-regulation of hematopoietic prostaglandin D2 synthase in macrophages is mediated through the activation of peroxisome proliferator-activated receptor (PPAR) gamma. *J Biol Chem*. 2011;286:27471-27482.

SUPPORTING INFORMATION

Additional Supporting Information may be found online in the Supporting Information section.

How to cite this article: Zhang Y, Yang X, Yan W, et al. Thymopentin improves the survival of septic mice by promoting the production of 15-deoxy-prostaglandin J2 and activating the PPARγ signaling pathway. *The FASEB Journal*. 2020;34:11772–11785. https://doi.org/10.1096/fj.202000467R